

# Magnetic order in the quasi-two-dimensional easy-plane XXZ model

D. Ihle

*Institut für Theoretische Physik, Universität Leipzig, D-04109 Leipzig, Germany*

C. Schindelin

*COI GmbH, Erlanger Strasse 62, D-91074 Herzogenaurach*

H. Fehske

*Physikalisches Institut, Universität Bayreuth, D-95440 Bayreuth, Germany*

(November 21, 2018)

A Green's-function theory of antiferromagnetic short-range and long-range order (LRO) in the  $S = 1/2$  quasi-two-dimensional easy-plane XXZ model is presented. As the main new result, *two* phase transitions due to the combined influence of spatial and spin anisotropy are found, where below the higher and lower Néel temperature there occurs LRO in the transverse and in both the transverse and longitudinal spin correlators, respectively. Comparing the theory with neutron-scattering data for the correlation length of  $\text{La}_2\text{CuO}_4$ , a very good agreement in the whole temperature dependence is obtained. Moreover, for  $\text{La}_2\text{CuO}_4$ ,  $\text{Sr}_2\text{CuO}_2\text{Cl}_2$ , and  $\text{Ca}_{0.85}\text{Sr}_{0.15}\text{CuO}_2$  the second phase with longitudinal LRO is predicted to appear far below room temperature.

PACS numbers: 75.10.-b, 75.10.Jm, 75.40.-s

## I. INTRODUCTION

To understand the unconventional behavior of high- $T_c$  superconductors, which is mainly ascribed to a strong antiferromagnetic (AFM) short-range order (SRO), the magnetic properties of the quasi-two-dimensional (2D) parent compounds were probed preferably by neutron scattering and NMR experiments, e.g., on  $\text{La}_2\text{CuO}_4$  [1–4],  $\text{Ca}_{0.85}\text{Sr}_{0.15}\text{CuO}_2$  [5],  $\text{YBa}_2\text{Cu}_3\text{O}_{6+x}$  ( $x \lesssim 0.4$ ) [6] and  $\text{L}_2\text{CuO}_4$  ( $L=\text{Nd, Pr}$ ) [7]. In particular, the staggered magnetization [1–3,5,6] and the AFM correlation length [2,4] were investigated. To analyze the experimental data, quasi-2D Heisenberg models including a weak spin anisotropy (easy-plane XXZ models) were considered [1–7] and treated by linear spin-wave theory [3,5,6] and a Schwinger-boson approach [1]. Recently, a quasi-2D anisotropic (easy-axis) Heisenberg model was studied within a boson-fermion mean-field theory [8]. However, those auxiliary-field approaches and most of the spin-wave theories for related spin models (for references to most of the early work, see Ref. [9]) yield reasonable results only at sufficiently low temperatures, since the temperature-dependent SRO is not adequately taken into account. To provide a good description of magnetic SRO at arbitrary temperatures, a Green's-function theory based on the projection method was developed for the spatially anisotropic Heisenberg models [9–11] and for the 1D [12] and 2D easy-plane XXZ models [13].

In this paper we extend our previous work to the  $S = 1/2$  quasi-2D easy-plane XXZ model

$$\mathcal{H} = \frac{J}{2} \left[ \sum_{\langle i,j \rangle_{x,y}} \left( S_i^+ S_j^- + \Delta S_i^z S_j^z \right) \right]$$

$$+ R_z \sum_{\langle i,j \rangle_z} \left( S_i^+ S_j^- + \Delta S_i^z S_j^z \right) \Big]. \quad (1)$$

Here,  $\langle i,j \rangle_{xy}$  and  $\langle i,j \rangle_z$  denote nearest-neighbor (NN) sites in the  $xy$  plane and along the  $z$  direction of a simple cubic lattice, respectively,  $R_z = J_z/J < 1$  describes the AFM interplane coupling (throughout we set  $J = 1$ ), and the spin anisotropy parameter  $\Delta$  is considered in the AFM region  $0 < \Delta \leq 1$ . In the limiting cases  $\Delta = 1$  and  $R_z = 0$  the model (1) reduces to the models studied in Refs. [9] and [13], respectively.

Our Green's-function theory outlined in the Appendix is based on an approximate time evolution of spin operators, e.g.,  $-\ddot{S}_{\mathbf{q}}^z = (\omega_{\mathbf{q}}^{zz})^2 S_{\mathbf{q}}^z$ , resulting from a decoupling of three-spin operator products which is improved by the introduction of vertex parameters. For the temperature dependence of some vertex parameters assumptions are made which are detailed and motivated in the Appendix. Within this theory we examine the combined effects of spatial and spin anisotropy on the AFM long-range order (LRO) at  $T = 0$  (Sec. II), the Néel transition temperature, and on the AFM correlation length (Sec. III). In Sec. IV we compare our results with experiments. For  $\text{La}_2\text{CuO}_4$ ,  $\text{Sr}_2\text{CuO}_2\text{Cl}_2$ , and  $\text{Ca}_{0.85}\text{Sr}_{0.15}\text{CuO}_2$  our theory predicts, in addition to the usual Néel transition, a further transition far below room temperature, where the spin correlators between the  $z$ -components start to develop AFM LRO.

## II. GROUND-STATE LONG-RANGE ORDER

Analyzing the magnetic LRO described by the staggered magnetizations  $m^\nu$  [ $\nu = \pm, zz$ ; cf. Eq. (11)] at  $T = 0$  as functions of  $R_z$  and  $\Delta$ , we obtain transverse

LRO in the whole parameter region considered and two solutions differing in the existence of longitudinal LRO. That is, we obtain a phase with  $m^{zz} = 0$  (phase I) and a phase with  $m^{zz} \neq 0$  (phase II), where in both phases we have  $m^{+-} \neq 0$ . The stabilization of longitudinal LRO in the easy-plane region by the interplane coupling may be due to the reduction of quantum spin fluctuations in higher dimensions.

In Fig. 1 the  $R_z - \Delta$  phase diagram is shown, where for  $R_z \neq 0$  the transition across the phase boundary denoted respectively by  $R_{z,c}(\Delta)$  and  $\Delta_c(R_z)$  is found to be of second order (cf. inset). Let us consider the phase transition in the vicinity of the critical point  $(\Delta, R_z) = (1, 0)$  in more detail. In our approach the solution for  $m^{zz}$  turns out to depend sensitively on the input data for  $\partial e(\Delta, 1)/\partial \Delta \equiv e'$  used to determine the vertex parameter  $\alpha_2^{zz}$ , where  $e(\Delta, 1)$  denotes the ground-state energy of the 2D XXZ model (see Appendix). Taking for  $e(\Delta, 1)$  the exact diagonalization (ED) data on lattices with up to 36 sites (without finite-size scaling) from Ref. [13], we obtain  $\lim_{R_z \rightarrow 0} \Delta_c(R_z) \equiv \Delta_0 = 0.958$ . On the other hand, taking the Monte Carlo (MC) data from Ref. [14], which have to be interpolated between the few available points  $\Delta = 0, \pm 0.5, \pm 1$ , we get  $\lim_{\Delta \rightarrow 1} R_{z,c}(\Delta) \equiv R_{z,0} = 4.08 \times 10^{-2}$ . However, as is well known, at  $R_z = 0$  there is no longitudinal LRO for  $0 < \Delta < 1$  which means that we must have  $\Delta_0 = 1$ . Moreover, we expect the interplane coupling to be a relevant perturbation with respect to the stabilization of LRO analogous to the situation in the 2D spatially anisotropic Heisenberg model [11,15], where LRO at a finite arbitrary small interchain coupling was found [15]. Therefore, we make the reasonable assumption  $R_{z,0} = 0$ . To fulfill the requirements  $\Delta_0 = 1$  and  $R_{z,0} = 0$  simultaneously, so that the phase boundary touches the critical point  $(\Delta, R_z) = (1, 0)$ , as input for  $e'$  we use a linear combination of the ED [13] and Monte Carlo data [14],  $e' = x e'_{ED} + (1-x)e'_{MC}$ . We find that the above requirements may be fulfilled, if  $x$  is chosen as  $x=0.44$ .

In the limit  $\Delta = 1$  we have rotational symmetry ( $C_{\mathbf{r}}^{zz} = C_{\mathbf{r}}^{+-}/2$ ), so that  $\sqrt{2}m^{zz}(R_z) = m^{+-}(R_z) \equiv \sqrt{2/3}m(R_z)$  with  $m$  defined as in Refs. [9–11]. In this limit, our result for  $m^{+-}(R_z)$  agrees with that of Ref. [9]. As can be seen in the inset, the effects of spin anisotropy on the longitudinal and transverse LRO are opposite: We have  $\partial m^{zz}/\partial \Delta > 0$ , whereas  $\partial m^{+-}/\partial \Delta < 0$  which agrees, at  $R_z = 0$ , with the Monte Carlo data [14] and the results of Ref. [13].

### III. FINITE-TEMPERATURE PROPERTIES

Considering the AFM LRO in the phases I and II [ $m^\nu(T=0) \neq 0$  at  $R_z > R_{z,c}$ ] at nonzero temperatures, the solution of the self-consistency equations (5), supplemented by the conditions for the vertex parameters [cf. Eqs. (12) and (15) to (17)], results in two second-

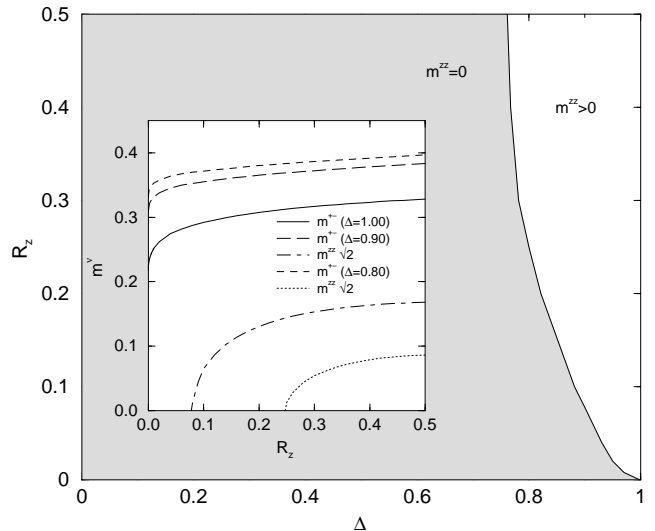


FIG. 1.:  $R_z - \Delta$  phase diagram and transverse and longitudinal zero-temperature magnetizations (inset) in the quasi-2D easy-plane XXZ model.

order phase transitions at  $T_N^{+-}(R_z, \Delta)$  and  $T_N^{zz}(R_z, \Delta)$  [ $m^\nu(T_N^\nu) = 0$ ] with  $T_N^{+-} > T_N^{zz}$  and  $T_N^{zz}(R_{z,c}) = 0$ . Figure 2 shows the Néel temperatures as functions of  $R_z$ , i.e., the  $T - R_z$  phase diagram for different spin anisotropies. For  $R_z = 0$  we obtain  $T_N^{+-} = 0$ , in agreement with the Mermin-Wagner theorem. At  $\Delta = 1$  we

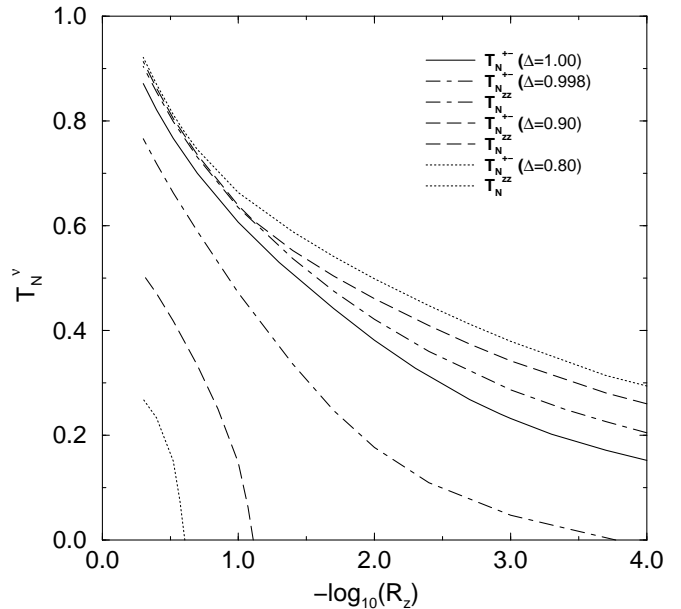


FIG. 2.:  $T - R_z$  phase diagram in the quasi-2D easy-plane XXZ model. Below the Néel temperature  $T_N^{zz}$  the phase with longitudinal long-range order becomes stable. The curves below the solid line belong to  $T_N^{zz}$ .

have  $T_N^{+-} = T_N^{zz} \equiv T_N$ . As compared with the results of Ref. [9], our values for  $T_N$  are somewhat higher (by about 9%) due to numerical uncertainties. On the other hand, in comparison with previous RPA and mean-field approaches (cf. Ref. [9]) our Néel temperatures are reduced by the improved description of SRO. For example, the  $T_N$  values found by the Schwinger-boson approach of Ref. [16] exceed our results by a factor of about 1.7 on the average.

Concerning the influence of spin anisotropy on the Néel transitions, we obtain  $\partial T_N^{+-}/\partial\Delta < 0$  and  $\partial T_N^{zz}/\partial\Delta > 0$ , corresponding to the  $\Delta$  dependence of  $m^\nu$  (cf. inset of Fig. 1). The dependence on  $\Delta$  of  $T_N^{+-}$  is in qualitative agreement with the behavior found in previous approaches [1,2]. There,  $T_N$  (being identified with  $T_N^{+-}$ ) is given as  $T_N/J = -2\pi M_0 \{\ln |4\alpha_{eff}/[\pi^2 M_0 \ln(4\alpha_{eff}/\pi)]\}^{-1}$  (Ref. [1]) with  $M_0 = 0.3$ ,  $\alpha_{eff} = 4\alpha_{xy} + 2R_z$ , and  $\alpha_{xy} = 1 - \Delta$  or as  $T_N/J = -4\pi\rho_S(\ln\alpha_{eff})^{-1}$  (Ref. [2]), where  $\rho_S$  is the spin stiffness. However, in contrast to those mean-field (Schwinger boson) results, in our theory the combined influence of spatial and spin anisotropy on  $T_N^{+-}$  cannot be expressed in terms of a single effective parameter. Considering the variations  $\delta R_z$  and  $\delta\alpha_{xy}$  under the condition  $\delta T_N^{+-} = 0$  we get  $\text{sgn}(\delta\alpha_{xy}) = -\text{sgn}(\delta R_z)$ . Whereas the  $T_N$  formulas quoted above yield  $\delta\alpha_{xy} = -\delta R_z/2$  for all  $R_z$ , from Fig. 2 we obtain a  $R_z$  dependent relation between  $\delta\alpha_{xy}$  and  $\delta R_z$ .

In Fig. 3, our numerical results for the temperature dependence of the magnetization  $m^\nu$  are depicted. They may be described by a  $T^2$  decrease at low enough temper-

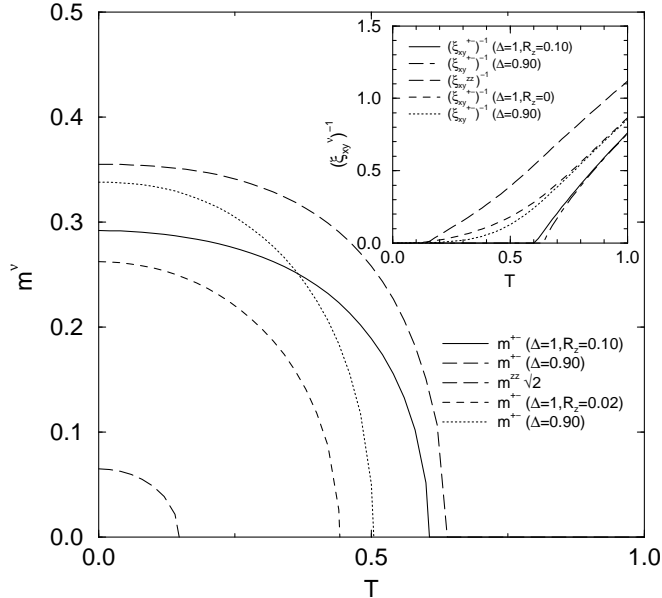


FIG. 3.: Staggered magnetizations versus temperature. The inset shows the inverse intraplane correlation lengths above the corresponding Néel temperatures.

atures (3D behavior) and by  $m^\nu(T) \propto (1 - T/T_N^\nu)^{1/2}$  for temperatures close to  $T_N^\nu$ , as was also found in the  $\Delta = 1$  limit [9]. The influence of spatial and spin anisotropy on  $m^\nu(T)$  is analogous to that on  $m^\nu(T = 0)$  shown in the inset of Fig. 1.

In the inset of Fig. 3 the inverse AFM intraplane correlation lengths above  $T_N^\nu$  are plotted, where the effects of the interplane coupling and spin anisotropy are visible. In the vicinity of  $T_N^{+-}$  the temperature dependence of  $(\xi_{xy}^{+-})^{-1}$  changes from an exponential law in the 2D case ( $T_N^{+-} = 0$ ) to a linear behavior for  $R_z > 0$ . Equally,  $(\xi_{xy}^{zz})^{-1}$  near  $T_N^{zz}$  behaves as  $T - T_N^{zz}$ . According to the influence of spin anisotropy on  $T_N^\nu$  we get  $\partial\xi_{xy}^{zz}/\partial\Delta > 0$  and  $\partial\xi_{xy}^{+-}/\partial\Delta < 0$ . The behavior of  $\xi_{xy}^{+-}$  qualitatively agrees with the anisotropy dependence of the mean-field expression for  $\xi$  (being identified with  $\xi_{xy}^{+-}$ ) given in Ref. [2],  $\xi = \xi_0(1 - \alpha_{eff}\xi_0^2)^{-1/2}$ , where  $\xi_0$  denotes the correlation length for  $R_z = 0$  and  $\Delta = 1$ .

Finally let us consider the heuristic relation between  $T_N^{+-}$  and the transverse 2D correlation length at  $T_N^{+-}$  which is often used in describing the experimental data [17] and is given by  $Q(R_z, \Delta = 1) = 0.25$  with  $Q(R_z, \Delta) \equiv R_z(T_N^{+-})^{-1}[m^{+-}(T = 0, R_z = 0, \Delta)\xi_{xy}^{+-}(T = T_N^{+-}, R_z = 0, \Delta)]^2$ . By our results,  $Q(R_z, \Delta)$  in the experimentally relevant region (cf. Sec. IV)  $2 \times 10^{-4} \leq R_z \leq 2 \times 10^{-2}$  and at  $\Delta = 1(0.8)$  is found to vary between 0.21 (0.31) and 0.095 (0.23). That is, the heuristic estimate is roughly confirmed by our theory.

#### IV. COMPARISON WITH EXPERIMENTS

Let us first compare our results for the transverse intraplane correlation length  $\xi_{xy}^{+-}$  with the neutron-scattering data on  $\text{La}_2\text{CuO}_4$  (Ref. [4]) in the range  $340 \text{ K} \leq T \leq 820 \text{ K}$  plotted in Fig. 4. Based on the 2D Heisenberg model ( $\Delta = 1$ ), in Ref. [18] the exchange energy  $J$  was determined by a least-squares fit ( $a = 3.79 \text{ \AA}$ ), where for our choice of the vertex parameters the realistic value  $J = 117 \text{ meV}$  was found. Here, we fix this value and consider the effects of spatial and spin anisotropy on  $\xi_{xy}^{+-}(T)$ . The deviation of the theory for  $R_z = 0$  and  $T < 550 \text{ K}$  from the experimental data may be reduced by the inclusion of the interplane coupling, since  $\xi_{xy}^{-1}(T_N) = 0$ . For  $\Delta = 1$  and  $T_N = 325 \text{ K}$  [1,4] we obtain  $R_z = 1.2 \times 10^{-3}$ , and the theoretical low-temperature  $\xi_{xy}^{-1}$  curve lies only somewhat above the experiments (cf. Fig. 4). Taking into account the spin anisotropy  $\alpha_{xy} = 1.5 \times 10^{-4}$  [2] or  $\alpha_{xy} = 5.7 \times 10^{-4}$  [4], for  $T_N^{+-} = 325 \text{ K}$  we get  $R_z = 3.0 \times 10^{-4}$ . For those parameters we obtain an excellent agreement between theory and experiment over the whole temperature region. Note that the theoretical curves for  $\alpha_{xy} = 2 \times 10^{-4}$  (cf. Fig. 4) and  $\alpha_{xy} = 2 \times 10^{-3}$  agree within the accuracy of drawing.

Concerning our prediction of phase II with longitudinal LRO in  $\text{La}_2\text{CuO}_4$ , for  $\alpha_{xy} = 1.5 \times 10^{-4}$  ( $5.7 \times 10^{-4}$ ) we obtain the longitudinal zero-temperature magnetic moment  $\mu^{zz} \equiv 2\mu_B m^{zz} = 6.6 \times 10^{-2} \mu_B$  ( $6.1 \times 10^{-2} \mu_B$ ) as compared with the transverse moment  $\mu^{+-} \equiv 2\mu_B m^{+-} = 0.55 \mu_B$ . For the Néel temperature we find  $T_N^{zz} = 2.6 \times 10^{-2} J$  ( $2.4 \times 10^{-2} J$ ) equally to  $T_N^{zz} = 35 \text{ K}$  ( $33 \text{ K}$ ) [ $J = 117 \text{ meV}$ ]. With regard to the experimental verification of the two phases, the magnitude of the longitudinal moment ( $\mu^{zz} \gtrsim 0.1 \mu^{+-}$ ) may be large enough to allow a separation between  $\mu^{zz}$  and  $\mu^{+-}$  by polarized neutron-scattering studies on single crystals of  $\text{La}_2\text{CuO}_4$  [19].

Next we consider the compound  $\text{Sr}_2\text{CuO}_2\text{Cl}_2$  which is the best experimental realization of an  $S = 1/2$  2D Heisenberg antiferromagnet, where  $J = 125 \pm 6 \text{ meV}$ ,  $\alpha_{xy} = 1.4 \times 10^{-4}$ , and  $T_N^{+-} = 256.5 \text{ K}$  [20]. Keeping  $T_N^{+-}$  and  $\alpha_{xy}$  fixed (we take  $\alpha_{xy} = 2 \times 10^{-4}$ , as for  $\text{La}_2\text{CuO}_4$ ) and choosing  $J = 125 \text{ meV}$ ,  $120 \text{ meV}$ , and  $110 \text{ meV}$ , we obtain the interplane coupling  $R_z = 2.0 \times 10^{-5}$ ,  $4.0 \times 10^{-5}$ , and  $1.0 \times 10^{-5}$ , respectively. On the average we have  $R_z \simeq 5 \times 10^{-5} \ll \alpha_{xy}$  in qualitative agreement with the estimate given in Ref. [20]. In Fig. 5 our results for the transverse intraplane correlation length ( $a = 3.967 \text{ \AA}$ ), where  $(\xi_{xy}^{+-})^{-1} \propto T - T_N^{+-}$  near the transition to phase I, are compared with the neutron-scattering data [20]. For  $J = 125 \text{ meV}$  we obtain a very good agreement between theory and experiment at low enough temperatures ( $T \lesssim 400 \text{ K}$ ), whereas for  $J = 110 \text{ meV}$  the agreement is good at higher temperatures.

The data on the predicted phase II in  $\text{Sr}_2\text{CuO}_2\text{Cl}_2$  calculated for  $J = 125 \text{ meV}$ ,  $120 \text{ meV}$ , and  $110 \text{ meV}$  are ob-

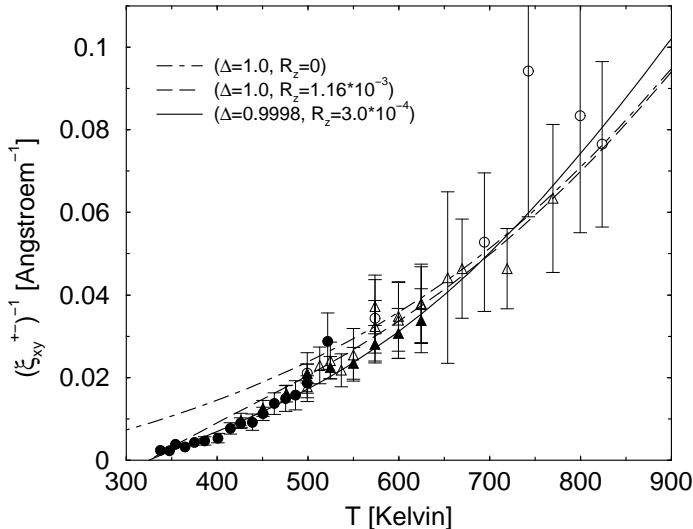


FIG. 4.: Inverse antiferromagnetic transverse intraplane correlation length in  $\text{La}_2\text{CuO}_4$  obtained by the neutron-scattering experiments of Ref. [4] (symbols) and from the theory for different spatial and spin anisotropies.

tained as  $\mu^{zz}/\mu_B = 2.8 \times 10^{-2}$ ,  $3.9 \times 10^{-2}$ , and  $5.5 \times 10^{-2}$  (for comparison,  $\mu^{+-}/\mu_B = 0.54$ ) and as  $T_N^{zz} = 7 \text{ K}$ ,  $12 \text{ K}$ , and  $18 \text{ K}$ , respectively. As in  $\text{La}_2\text{CuO}_4$ , the magnitude of the longitudinal moment ( $\mu^{zz} \simeq 4 \times 10^{-2} \mu_B \simeq 0.08 \mu^{+-}$ ) may be large enough to be detected by polarized neutron-scattering experiments on  $\text{Sr}_2\text{CuO}_2\text{Cl}_2$  single crystals.

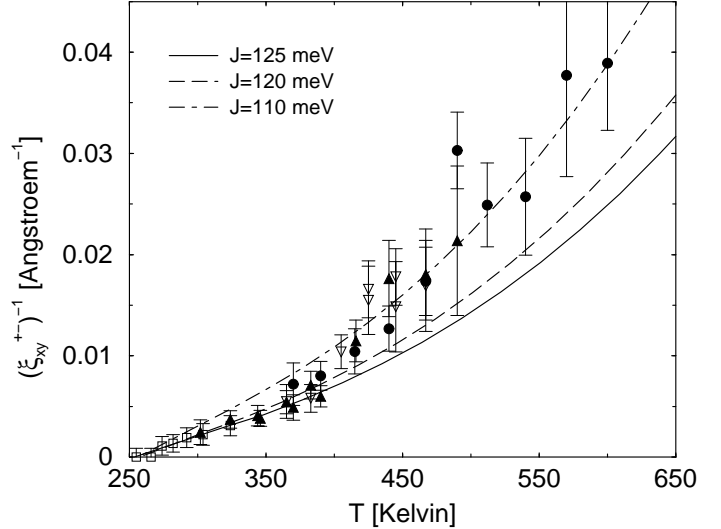


FIG. 5.: Inverse antiferromagnetic transverse intraplane correlation length in  $\text{Sr}_2\text{CuO}_2\text{Cl}_2$  obtained by the neutron-scattering experiments of Ref. [20] (symbols) and from the theory for different exchange energies  $J$ .

Considering  $\text{Ca}_{0.85}\text{Sr}_{0.15}\text{CuO}_2$  ( $T_N = 540 \text{ K}$  and  $J = 125 \text{ meV}$  [5]), for  $\Delta = 1$  we obtain  $R_z = 9.0 \times 10^{-3}$  as compared with  $R_z \simeq 2.5 \times 10^{-2}$  resulting from a fit of the magnetization data [5]. Taking  $\alpha_{xy}$  as for  $\text{La}_2\text{CuO}_4$ ,  $\alpha_{xy} = 1.5 \times 10^{-4}$  [5], we get  $R_z = 5.0 \times 10^{-3}$ . For the zero-temperature magnetic moments and the Néel temperature we obtain  $\mu^{zz} = 0.16 \mu_B$ ,  $\mu^{+-} = 0.57 \mu_B$  and  $T_N^{zz} = 190 \text{ K}$ , respectively. Note that the longitudinal moment is more than twice as large ( $\mu^{zz} = 0.28 \mu^{+-}$ ) as in  $\text{La}_2\text{CuO}_4$ . However, contrary to  $\text{La}_2\text{CuO}_4$  and  $\text{Sr}_2\text{CuO}_2\text{Cl}_2$ , for  $\text{Ca}(\text{Sr})\text{CuO}_2$  single crystals are not available, so that neutron-scattering data do not exist until now [19].

## V. SUMMARY

In this paper we presented a Green's-function theory for the quasi-2D easy-plane XXZ model allowing the calculation of all static magnetic properties at arbitrary temperatures, where we focused on the effects of spatial and spin anisotropy on the AFM LRO and the correlation length. As a qualitatively new result, for appropriate model parameters we obtained two phase transitions, where the paramagnetic phase with pronounced AFM SRO becomes unstable against a phase with transverse LRO only and, at a lower temperature, a phase with both transverse and longitudinal LRO. Comparing the theory with neutron-scattering experiments on the correlation length of  $\text{La}_2\text{CuO}_4$ , an excellent agreement is found. Furthermore, the second Néel transition (to the phase with longitudinal LRO) in  $\text{La}_2\text{CuO}_4$ ,  $\text{Sr}_2\text{CuO}_2\text{Cl}_2$ , and  $\text{Ca}_{0.85}\text{Sr}_{0.15}\text{CuO}_2$  is predicted to occur at about 30 K, 10 K, and 190 K, respectively. Our goal is to stimulate a wider discussion and new experiments in this direction.

*Acknowledgments.* The authors are greatly indebted to B. Keimer and R. Hayn for stimulating discussions.

### APPENDIX: THEORY OF SPIN SUSCEPTIBILITY

The spin susceptibilities  $\chi_{\mathbf{q}}^{+-}(\omega) = -\langle\langle S_{\mathbf{q}}^+; S_{-\mathbf{q}}^- \rangle\rangle_{\omega}$  and  $\chi_{\mathbf{q}}^{zz}(\omega) = -\langle\langle S_{\mathbf{q}}^z; S_{-\mathbf{q}}^z \rangle\rangle_{\omega}$ , ( $\langle\langle \dots; \dots \rangle\rangle_{\omega}$  denotes the two-time retarded commutator Green's function) are determined by the projection method taking, as for the XXZ chain [12], the basis  $(S_{\mathbf{q}}^+, i\dot{S}_{\mathbf{q}}^+)$  and  $(S_{\mathbf{q}}^z, i\dot{S}_{\mathbf{q}}^z)$ , respectively. We obtain

$$\chi_{\mathbf{q}}^{\nu}(\omega) = -\frac{M_{\mathbf{q}}^{\nu}}{\omega^2 - (\omega_{\mathbf{q}}^{\nu})^2}; \quad \nu = +-, zz, \quad (2)$$

with the first spectral moments  $M_{\mathbf{q}}^{+-} = \langle\langle i\dot{S}_{\mathbf{q}}^+, S_{-\mathbf{q}}^- \rangle\rangle$  and  $M_{\mathbf{q}}^{zz} = \langle\langle i\dot{S}_{\mathbf{q}}^z, S_{-\mathbf{q}}^z \rangle\rangle$  given by the exact expressions

$$M_{\mathbf{q}}^{+-} = -4[C_{1,0,0}^{+-}(1 - \Delta\gamma_{\mathbf{q}}) + 2C_{1,0,0}^{zz}(\Delta - \gamma_{\mathbf{q}})] \quad (3)$$

$$-2R_z[C_{0,0,1}^{+-}(1 - \Delta \cos q_z) + 2C_{0,0,1}^{zz}(\Delta - \cos q_z)]$$

$$M_{\mathbf{q}}^{zz} = -4C_{1,0,0}^{+-}(1 - \gamma_{\mathbf{q}}) - 2R_z C_{0,0,1}^{+-}(1 - \cos q_z), \quad (4)$$

$C_{nml}^{\nu} \equiv C_{\mathbf{r}}^{\nu}$ ,  $C_{\mathbf{r}}^{+-} = \langle S_0^+ S_{\mathbf{r}}^- \rangle$ ,  $C_{\mathbf{r}}^{zz} = \langle S_0^z S_{\mathbf{r}}^z \rangle$ ,  $\mathbf{r} = n\mathbf{e}_x + m\mathbf{e}_y + l\mathbf{e}_z$ , and  $\gamma_{\mathbf{q}} = (\cos q_x + \cos q_y)/2$ . The spin correlators are calculated as

$$C_{\mathbf{r}}^{\nu} = \frac{1}{N} \sum_{\mathbf{q}} \frac{M_{\mathbf{q}}^{\nu}}{2\omega_{\mathbf{q}}^{\nu}} [1 + 2p(\omega_{\mathbf{q}}^{\nu})] e^{i\mathbf{q}\mathbf{r}}, \quad (5)$$

where  $p(\omega_{\mathbf{q}}^{\nu}) = (e^{\omega_{\mathbf{q}}^{\nu}/T} - 1)^{-1}$ . The NN correlation functions are related to the internal energy per site  $\varepsilon = 2(C_{1,0,0}^{+-} + \Delta C_{1,0,0}^{zz}) + R_z(C_{0,0,1}^{+-} + \Delta C_{0,0,1}^{zz})$ .

The spectra  $\omega_{\mathbf{q}}^{\nu}$  are calculated in the approximations  $-\dot{S}_{\mathbf{q}}^+ = (\omega_{\mathbf{q}}^{+-})^2 S_{\mathbf{q}}^+$  and  $-\dot{S}_{\mathbf{q}}^z = (\omega_{\mathbf{q}}^{zz})^2 S_{\mathbf{q}}^z$ , where products of three spin operators in  $-\dot{S}_i^+$  and  $-\dot{S}_i^z$  along

NN sequences  $\langle i, j, l \rangle$  are decoupled. Introducing vertex parameters in the spirit of the scheme by Shimahara and Takada [21] and extending the decouplings given in Refs. [11,9,12], we have

$$S_i^+ S_j^+ S_l^- = \alpha_{1x,1z}^{+-} \langle S_j^+ S_l^- \rangle S_i^+ + \alpha_2^{+-} \langle S_i^+ S_l^- \rangle S_j^+, \quad (6)$$

$$S_i^z S_j^+ S_l^- = \alpha_{1x,1z}^{zz} \langle S_j^+ S_l^- \rangle S_i^z, \quad (7)$$

$$S_i^+ S_j^z S_l^- = \alpha_2^{zz} \langle S_i^+ S_l^- \rangle S_j^z. \quad (8)$$

Here,  $\alpha_{1x}^{\nu}$  and  $\alpha_{1z}^{\nu}$  are attached to NN correlations in the  $xy$ -plane and along the  $z$  direction, respectively, and  $\alpha_2^z$  is associated with longer ranged correlation functions. We obtain

$$\begin{aligned} (\omega_{\mathbf{q}}^{+-})^2 = & [1 + 2\alpha_2^{+-}(C_{2,0,0}^{+-} + 2C_{1,1,0}^{+-})](1 - \Delta\gamma_{\mathbf{q}}) \\ & + \Delta[1 + 4\alpha_2^{+-}(C_{2,0,0}^{zz} + 2C_{1,1,0}^{zz})](\Delta - \gamma_{\mathbf{q}}) \\ & + 2\alpha_{1x}^{+-} C_{1,0,0}^{+-} [\Delta(4\gamma_{\mathbf{q}}^2 - 1) - 3\gamma_{\mathbf{q}}] \\ & + 4\alpha_{1x}^{+-} C_{1,0,0}^{zz} [4\gamma_{\mathbf{q}}^2 - 1 - 3\Delta\gamma_{\mathbf{q}}] \\ & + \frac{R_z^2}{2} \left[ (1 + 2\alpha_2^{+-} C_{0,0,2}^{+-})(1 - \Delta \cos q_z) \right. \\ & + \Delta(1 + 4\alpha_2^{+-} C_{0,0,2}^{zz})(\Delta - \cos q_z) \\ & + 2\alpha_{1z}^{+-} C_{0,0,1}^{+-} (\Delta \cos 2q_z - \cos q_z) \\ & \left. + 4\alpha_{1z}^{+-} C_{0,0,1}^{zz} (\cos 2q_z - \Delta \cos q_z) \right] \\ & 2R_z \left[ 2\alpha_2^{+-} C_{1,0,1}^{+-} (2 - \Delta\gamma_{\mathbf{q}} - \Delta \cos q_z) \right. \\ & + 4\alpha_2^{+-} C_{1,0,1}^{zz} \Delta (2\Delta - \gamma_{\mathbf{q}} - \cos q_z) \\ & + 2\alpha_{1z}^{+-} C_{0,0,1}^{+-} \gamma_{\mathbf{q}} (\Delta \cos q_z - 1) \\ & + 4\alpha_{1z}^{+-} C_{0,0,1}^{zz} \gamma_{\mathbf{q}} (\cos q_z - \Delta) \\ & \left. + 2\alpha_{1x}^{+-} C_{1,0,0}^{+-} \cos q_z (\Delta\gamma_{\mathbf{q}} - 1) \right. \\ & \left. + 4\alpha_{1x}^{+-} C_{1,0,0}^{zz} \cos q_z (\gamma_{\mathbf{q}} - \Delta) \right], \quad (9) \end{aligned}$$

$$\begin{aligned} (\omega_{\mathbf{q}}^{zz})^2 = & 2(1 - \gamma_{\mathbf{q}}) \left[ 1 + 2\alpha_2^{zz} (C_{2,0,0}^{+-} + 2C_{1,1,0}^{+-}) \right. \\ & \left. - 2\Delta\alpha_{1x}^{zz} C_{1,0,0}^{+-} (1 + 4\gamma_{\mathbf{q}}) \right] \\ & + R_z^2 (1 - \cos q_z) \left[ 1 + 2\alpha_2^{zz} C_{0,0,2}^{+-} \right. \\ & \left. - 2\Delta\alpha_{1z}^{zz} C_{0,0,1}^{+-} (1 + 2\cos q_z) \right] \\ & + 8R_z \left[ \alpha_2^{zz} C_{1,0,1}^{+-} (2 - \gamma_{\mathbf{q}} - \cos q_z) \right. \\ & + \Delta\alpha_{1z}^{zz} C_{0,0,1}^{+-} \gamma_{\mathbf{q}} (\cos q_z - 1) \\ & \left. + \Delta\alpha_{1x}^{zz} C_{1,0,0}^{+-} \cos q_z (\gamma_{\mathbf{q}} - 1) \right]. \quad (10) \end{aligned}$$

Note that in the special cases  $R_z = 0$  and  $\Delta = 1$  the spectra reduce to the expressions given in Refs. [13] and [9], respectively.

The LRO in the correlators  $C_{\mathbf{r}}^{\nu}$  is reflected in our theory by the closure of the spectrum gap at  $\mathbf{Q} = (\pi, \pi, \pi)$  as  $T$  approaches  $T_N^{\nu}$  from above, so that  $\lim_{T \rightarrow T_N^{\nu}} (\chi_{\mathbf{Q}}^{\nu})^{-1} = 0$  and  $\omega_{\mathbf{Q}}^{\nu} = 0$  at  $T \leq T_N^{\nu}$ . Separating the condensation part  $C^{\nu} e^{i\mathbf{Q}\mathbf{r}}$  from  $C_{\mathbf{r}}^{\nu}$  [cf. Eq. (5)], the magnetization  $m^{\nu}$  is calculated as

$$(m^{\nu})^2 = \frac{1}{N} \sum_{\mathbf{r}} C_{\mathbf{r}}^{\nu} e^{-i\mathbf{Q}\mathbf{r}} = C^{\nu}. \quad (11)$$

Considering the uniform static longitudinal susceptibility  $\chi_0^{zz} = \lim_{\mathbf{q} \rightarrow 0} M_{\mathbf{q}}^{zz} / (\omega_{\mathbf{q}}^{zz})^2$ , the ratio of the anisotropic functions  $M_{\mathbf{q}}^{zz}$  and  $(\omega_{\mathbf{q}}^{zz})^2 = c_{xy}^2(q_x^2 + q_y^2) + c_z^2 q_z^2$  must be isotropic in the limit  $\mathbf{q} \rightarrow 0$ . This yields the condition

$$(c_z/c_{xy})^2 = R_z C_{0,0,1}^{+-} / C_{1,0,0}^{+-} \quad (12)$$

with the squared spin-wave velocities

$$c_{xy}^2 = \frac{1}{2} + \alpha_2^{zz} (C_{2,0,0}^{+-} + 2C_{1,1,0}^{+-}) - 5\Delta \alpha_{1x}^{zz} C_{1,0,0}^{+-} + 2R_z (\alpha_2^{zz} C_{1,0,1}^{+-} - \Delta \alpha_{1z}^{zz} C_{1,0,0}^{+-}), \quad (13)$$

$$c_z^2 = R_z^2 \left( \frac{1}{2} + \alpha_2^{zz} C_{0,0,2}^{+-} - 3\Delta \alpha_{1z}^{zz} C_{0,0,1}^{+-} \right) + 4R_z (\alpha_2^{zz} C_{1,0,1}^{+-} - \Delta \alpha_{1z}^{zz} C_{0,0,1}^{+-}). \quad (14)$$

Concerning the vertex parameters in our self-consistency scheme, three parameters are fixed by the sum rules  $C_0^{+-} = 1/2$ ,  $C_0^{zz} = 1/4$ , and by Eq. (12) for all  $T$ . To determine the free parameters taken as  $\alpha_{1x,1z}^{+-}$  and  $\alpha_2^{zz}$ , we need additional conditions. Let us consider the ground-state energy per site which we compose approximately, following Ref. [9], as  $\varepsilon(\Delta, R_z) = e(\Delta, R_z) + e(\Delta, 1) - e(\Delta, 0)$ . Here,  $e(\Delta, R_z)$  denotes the ground-state energy of the 2D spatially anisotropic XXZ model [Eq. (1) without sum in  $y$  direction], where the values in the 1D ( $R_z = 0$ ) and 2D cases ( $R_z = 1$ ) are taken from Ref. [22] and the exact data of Refs. [13,14], respectively. Since  $e(\Delta, R_z)$  is known for  $R_z = 0, 1$  and  $\Delta = 1$  (taken from the Ising-expansion results by Affleck et al. [23]), we approximate  $e(\Delta, R_z)$  by the linear interpolation  $e(\Delta, R_z) = e(\Delta, 0) + [e(\Delta, 1) - e(\Delta, 0)][e(1, 1) - e(1, 0)]^{-1}[e(1, R_z) - e(1, 0)]$ . At  $T = 0$ , we adjust  $\alpha_{1x}^{+-}$  to  $\varepsilon(\Delta, R_z)$  and  $\alpha_2^{zz}$  to  $\partial \varepsilon / \partial \Delta = 2C_{1,0,0}^{zz} + R_z C_{0,0,1}^{zz}$ .

To formulate conditions for  $\alpha_{1x}^{+-}$  and  $\alpha_2^{zz}$  also at finite temperatures, we follow the reasonings of Refs. [21,10,12]. That means, we conjecture that the ‘‘vertex corrections’’  $\alpha_{1x}^{\nu}(T) - 1$  and  $\alpha_2^{zz}(T) - 1$  have similar temperature dependences and vanish in the high- $T$  limit. Correspondingly, as the simplest interpolation between high temperatures and  $T = 0$  we assume the ratio of two vertex corrections as temperature independent and fixed by the ground-state value, i.e.,

$$\frac{\alpha_{1x}^{+-}(T) - 1}{\alpha_{1x}^{zz}(T) - 1} = \text{const.} \quad (15)$$

$$\frac{\alpha_2^{zz}(T) - 1}{\alpha_{1x}^{zz}(T) - 1} = \text{const.} \quad (16)$$

To determine  $\alpha_{1z}^{+-}(T)$ , as compared with  $\alpha_{1z}^{zz}(T)$  fixed by the ‘‘isotropy condition’’ (12) resulting from  $\chi_0^{zz}$ , we first note that an analogous condition cannot be derived from  $\chi_0^{+-} = \lim_{\mathbf{q} \rightarrow 0} M_{\mathbf{q}}^{+-} / (\omega_{\mathbf{q}}^{+-})^2$ , since both  $M_{\mathbf{q}}^{(1)}$  and  $\omega_{\mathbf{q}}^{+-}$  have non-zero  $\mathbf{q} \rightarrow 0$  limits [cf. Eqs. (3) and (9)]. Therefore, for  $\alpha_{1z}^{+-}(T)$  we make the plausible ansatz assuming the ratio  $\alpha_{1z}^{\nu}(T) / \alpha_{1x}^{\nu}(T)$  as  $\nu$  independent, i.e.,

$$\frac{\alpha_{1z}^{+-}(T)}{\alpha_{1x}^{+-}(T)} = \frac{\alpha_{1z}^{zz}(T)}{\alpha_{1x}^{zz}(T)}. \quad (17)$$

From the solution of the self-consistency equations the AFM correlation lengths above  $T_N^{\nu}$  may be evaluated. They are obtained by the expansion of  $\chi_{\mathbf{q}}^{\nu}$  around  $\mathbf{Q}$ ,  $\chi_{\mathbf{q}}^{\nu} = \chi_{\mathbf{Q}}^{\nu} [1 + (\xi_{xy}^{\nu})^2 (k_x^2 + k_y^2) + (\xi_z^{\nu})^2 k_z^2]^{-1}$  with  $\mathbf{k} = \mathbf{q} - \mathbf{Q}$ . The squared intraplane correlation lengths are given by

$$(\xi_{xy}^{+-})^2 = -(\omega_{\mathbf{Q}}^{+-})^{-2} \quad (18)$$

$$\begin{aligned} & \times \left[ \frac{\Delta}{2} + \Delta \alpha_2^{+-} \left( \frac{1}{2} C_{2,0,0}^{+-} + C_{2,0,0}^{zz} + C_{1,1,0}^{+-} + 2C_{1,1,0}^{zz} \right) \right. \\ & + \alpha_{1x}^{+-} \left( (4\Delta + \frac{3}{2}) C_{1,0,0}^{+-} + (8 + 3\Delta) C_{1,0,0}^{zz} \right) \\ & + R_z \left[ \alpha_{1x}^{+-} (\Delta C_{1,0,0}^{+-} + 2C_{1,0,0}^{zz}) + \alpha_{1z}^{+-} (C_{0,0,1}^{+-} + 2C_{0,0,1}^{zz}) \right. \\ & \left. \left. + \Delta (\alpha_{1z}^{+-} (C_{0,0,1}^{+-} + 2C_{0,0,1}^{zz}) + \alpha_2^{+-} (C_{1,0,1}^{+-} + 2C_{1,0,1}^{zz})) \right) \right] \\ & - (\Delta C_{1,0,0}^{+-} + 2C_{1,0,0}^{zz}) / M_{\mathbf{Q}}^{+-}, \end{aligned}$$

$$(\xi_{xy}^{zz})^2 = -(\omega_{\mathbf{Q}}^{zz})^{-2} \quad (19)$$

$$\begin{aligned} & \times \left[ \frac{1}{2} + \alpha_2^{zz} (C_{2,0,0}^{+-} + 2C_{1,1,0}^{+-}) + 11\Delta \alpha_{1x}^{zz} C_{1,0,0}^{+-} \right. \\ & \left. + 2R_z (\alpha_{1x}^{zz} \Delta C_{1,0,0}^{+-} + 2\alpha_{1z}^{zz} \Delta C_{0,0,1}^{+-} + \alpha_2^{zz} C_{1,0,1}^{+-}) \right] \\ & - 2C_{1,0,0}^{+-} / M_{\mathbf{Q}}^{zz}. \end{aligned}$$

- 
- [1] B. Keimer, A. Aharony, A. Auerbach, R. J. Birgeneau, A. Cassanho, Y. Endoh, R. W. Erwin, M. A. Kastner, and G. Shirane, Phys. Rev. B **45**, 7430 (1992).
  - [2] B. Keimer, N. Belk, R. J. Birgeneau, A. Cassanho, C. Y. Chen, M. Greven, M. A. Kastner, A. Aharony, Y. Endoh, R. W. Erwin, and G. Shirane, Phys. Rev. B **46**, 14034 (1992).
  - [3] M. Matsumura, M. Mali, J. Roos, and D. Brinkmann, Phys. Rev. B **56**, 8938 (1997).
  - [4] R. J. Birgeneau, M. Greven, M. A. Kastner, Y. S. Lee, B. O. Wells, Y. Endoh, K. Yamada, and G. Shirane, Phys. Rev. B **59**, 13788 (1999).
  - [5] M. Matsumura, F. Raffa, and D. Brinkmann, Phys. Rev. B **60**, 6285 (1999); A. Lombardi, M. Mali, J. Roos, D. Brinkmann, and I. Mangelschots, Phys. Rev. B **54**, 93 (1996).
  - [6] M. Matsumura, S. Nishiyama, Y. Iwamoto, and Y. Yamagata, J. Phys. Soc. Jpn. **62**, 4081 (1993); J. M. Tranquada, G. Shirane, B. Keimer, S. Shamoto, and M. Sato, Phys. Rev. B **40**, 4053 (1989).

- [7] M. Matsuda, K. Yamada, K. Kakurai, H. Kadowaki, T. R. Thurston, Y. Endoh, Y. Hidaka, R. J. Birgeneau, M. A. Kastner, P. M. Gehring, A. H. Moudden, and G. Shirane, *Phys. Rev. B* **42**, 10098 (1990).
- [8] V. Yu. Irkhin, A. A. Katanin, and M. I. Katsnelson, *Phys. Rev. B* **60**, 1082 (1999).
- [9] L. Siurakshina, D. Ihle, and R. Hayn, *Phys. Rev. B* **61**, 14601 (2000).
- [10] S. Winterfeldt and D. Ihle, *Phys. Rev. B* **56**, 5535 (1997); *ibid* **59**, 6010 (1999).
- [11] D. Ihle, C. Schindelin, A. Weiße, and H. Fehske, *Phys. Rev. B* **60**, 9240 (1999).
- [12] C. Schindelin, H. Fehske, H. Büttner, and D. Ihle, *Phys. Rev. B* **62**, 12141 (2000).
- [13] H. Fehske, C. Schindelin, A. Weiße, H. Büttner, and D. Ihle, *Brazil. Jour. Phys.* **30**, 720 (2000).
- [14] Y. Okabe and M. Kikuchi, *J. Phys. Soc. Jpn.* **57**, 4351 (1988).
- [15] A. W. Sandvik, *Phys. Rev. Lett.* **83**, 3069 (1999).
- [16] P. Kopietz, *Phys. Rev. Lett.* **68**, 3480 (1992).
- [17] S. Chakravarty, B. I. Halperin, and D. R. Nelson, *Phys. Rev. Lett.* **60**, 1057 (1988); *Phys. Rev. B* **39**, 2344 (1989).
- [18] S. Winterfeldt and D. Ihle, *Phys. Rev. B* **58**, 9402 (1998).
- [19] B. Keimer, private communication.
- [20] M. Greven, R. J. Birgeneau, Y. Endoh, M. A. Kastner, M. Matsuda, and G. Shirane, *Z. Phys. B* **96**, 465 (1995); M. Greven, R. J. Birgeneau, Y. Endoh, M. A. Kastner, B. Keimer, M. Matsuda, G. Shirane, and T. R. Thurston, *Phys. Rev. Lett.* **72**, 1096 (1994).
- [21] H. Shimahara and S. Takada, *J. Phys. Soc. Jpn.* **60**, 2394 (1991); *ibid* **61**, 989 (1992).
- [22] C. N. Yang and C. P. Yang, *Phys. Rev.* **150**, 321 (1966); *ibid* 327 (1966).
- [23] I. Affleck, M. P. Gelfand, and R. R. P. Singh, *J. Phys. A* **27**, 7313 (1994).